Investigation of Electrochemical Gas Generation in Ion Electrospray Thrusters

Investigation of Electrochemical Gas Generation in Ion Electrospray Thrusters

IEPC-2024-511

Presented at the 38th International Electric Propulsion Conference, Toulouse, France
June 23-28, 2024

Saba Z. Shaik* and Paulo C. Lozano†
Massachusetts Institute of Technology, Cambridge, MA, 02139, USA

This work investigates the electrochemical formation of gas-phase species in passively-fed ion electrospray thrusters biased with porous distal electrodes. Volatile reaction products of the ionic liquid propellants EMI-BF_4, EMI-Im, and EMI-CF_3BF_3 are identified using differential electrochemical mass spectrometry. Trace amounts of the same species are independently detected in tests of the electrospray thrusters, where gas appears to be generated at the distal electrode site after 6 hour periods of continuous emission at a beam current of about 200 μA. We find that higher beam currents, smaller electrodes, and single-polarity emission results in more gas being produced. No solid-phase products or hardware damage are observed in any of these tests. These findings suggest that electrochemistry could be an important efficiency loss in ion electrospray thrusters, even when no visible degradation occurs.

I. Introduction

Ion electrospray thrusters are a precise, miniature type of electric space propulsion that evaporate and accelerate charged particles from ionic liquid propellants using an applied electric field. In order to harness the many advantages that electrosprays offer in spacecraft applications, it is critical to improve their lifetime and reliability. One potential life-limiting mechanism is the electrochemical degradation of thruster hardware and propellant during long-duration firing. Adverse electrochemical reactions were observed in earlier work with externally-wetted single electrospray emitters,[1–3] but have not been studied in full electrospray propulsion systems that have been developed and matured in recent years.[4,5] This work aims to characterize electrochemical reactions and their primary influencers in MIT's microfabricated ion Electrospray Propulsion System (iEPS) with a focus on the formation of gas-phase reaction products.

Electrochemical reactions can diminish the lifetime and performance of ionic liquid ion sources through the formation of gaseous or solid-phase reaction products or degradation of the emitter material from energy released through the reactions. Several methods have been adopted in electrospray systems to mitigate these effects. First, the use of dielectric materials helps to preserve emitter tips from degradation, chemical or otherwise. Electrochemical damage has been observed on numerous occasions for metallic emitters,[1–3,6] but has not been reported for emitters made from borosilicate glass. Secondly, reversing the polarity of the applied firing voltage at a low frequency should deplete charge buildup thought to trigger electrochemical reactions.[1] Finally, the use of a distal electrode contact to polarize the propellant should constrain electrochemical reactions to the electrode surface, thus preserving the emission source.[7]

These strategies appear to be effective at preventing severe emitter damage based on visual inspections of thruster hardware after long-duration iEPS testing.[8,9] However, a more precise, in-situ method of detecting electrochemical reactions is needed to determine whether they occur during thruster operation. The most common techniques of examining electrochemical reactions (e.g. impedance spectroscopy, cyclic voltammetry) rely on precise measurements of Faradaic current through a probe electrode. This approach is not

*Ph.D. Candidate, Department of Aeronautics and Astronautics, sshaik@mit.edu.
†Professor, Department of Aeronautics and Astronautics, plozano@mit.edu.

suitable for an electrospray source, where any Faradaic current drawn from the electrode would be indistinguishable from emitted beam current. Alternatively, electrochemical reactions may be detected using mass spectrometry, in which the presence of specific species (i.e. reaction products) in a system indicates that a reaction has occurred. However, the electrochemical decomposition reactions of ionic liquids commonly used as electrospray propellants are not well understood. Different reaction pathways and products can be possible due to the size, composition, and complexity of the ion monomers, among other factors.[10,11] As such, these reactions need to be studied and characterized before they can be detected in electrospray thruster testing.

In this work, we seek to investigate electrochemical reactions in ion electrospray thrusters with a focus on the formation of volatile reaction products. We follow an approach called differential electrochemical mass spectrometry, where the electrochemical decomposition of electrospray propellants is induced using an electrochemical cell while a residual gas analyzer mass spectrometer is used to identify reaction products in-situ. This method has been used to study reactions in a wide range of media, including ionic liquids.[12,13] Then, we attempt to detect the same species in independent tests of iEPS thrusters. Finally, we explore the influencers of electrochemistry in electrospray systems by individually varying the distal electrode geometry, firing polarity, and beam current in a suite of thruster tests.

II. Electrochemistry in Ionic Liquid Ion Sources

Electrochemical reactions involve an exchange of electrons between species. In ionic liquid ion sources, these reactions are thought to be triggered when an *electrical double-layer* structure saturates with charge.[14] A double-layer consists of adjacent layers of opposite charge formed at the interface between an electronic conductor (electrode) and an ionic conductor (electrolyte), as shown in Figure 1. In an electrospray thruster, the electrode is the high-voltage contact used to polarize the propellant. Net charge on the electrode repels co-ions and attracts counterions in the ionic liquid. As current is drawn during ion emission, the surface charge on the electrode increases, prompting an increase in the counter-ion charge. Strong electric fields exist across the electrode-electrolyte interface since the distance between regions of opposite charge is approximately the size of a molecule. At a critical field strength, electron transfer across the interface is induced, consuming electrolyte and/or electrode material in a Faradaic reaction. The corresponding critical potential difference is called the *electrochemical window* (EW) of the medium. Many aqueous solutions have windows below 1.229 V, the standard potential for water electrolysis. Ionic liquids are solvent-free and thus have relatively large, symmetric electrochemical windows of about 4-6 V.[15,16] The physiochemical properties of several ionic liquids commonly used in electrospray propulsion applications[4,17,18] are provided in Table 1.

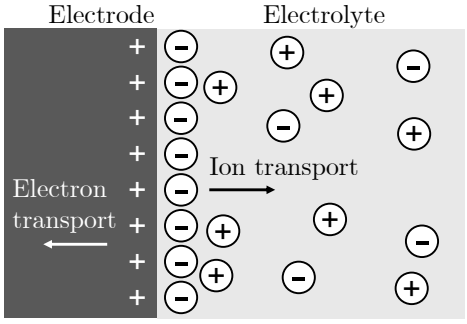

Figure 1. Electrical double layer formation across a positively charged electrode.

Table 1. Physiochemical properties of common ionic liquid propellants obtained from Ref.[16]

	EW [V]	Density [g/cm^3]	Melting Point [K]	Conductivity [S/m]	Viscosity [cP]
EMI-BF_4	4.55	1.28	287.57	1.36	42
EMI-CF_3BF_3	4.63	1.35	253.15	1.48	26
EMI-Im	4.59	1.52	256.15	0.92	34

The behavior of double-layers in systems with flat electrode geometries and dilute electrolytes is sometimes estimated using the Helmholtz-Perrin model, where the double-layer acts as a parallel-plate capacitor with constant capacitance.[1] Equation 1 gives the time t required for the double layer to breach its electrochemical window V_w, where I is the current, A is the active area of the electrode, δ is the distance between layers of charge, ε is the dielectric constant of the medium, and ε_0 is the permittivity of vacuum.

$$t = \varepsilon\varepsilon_0 \frac{V_w}{I} \frac{A}{\delta} \tag{1}$$

This simple model provides useful qualitative insights into the parameters that govern double-layer charging. However, the picture is generally not representative of electrospray thruster architectures, in which highly charged electrolytes (i.e. ionic liquids) and porous electrodes are often employed. Porous materials are used as supercapacitors in many industrial applications due to the large specific surface area available within them to store charge. Transport and charge-transfer processes in porous electrodes are very different than for flat electrodes, and high-fidelity models that include concentrated electrolytes tend to be prohibitively complex.[19,20] Simplified "transmission line" frameworks have been derived,[2] but deviate significantly from experimental measurements.[14] In summary, the onset of electrochemistry in ion electrospray thrusters is not well-predicted by existing models, but it is expected to be influenced by the distal electrode geometry, beam current, and properties of the propellant.

III. Methods

Test facilities, diagnsotics, and electrospray thruster units available in MIT's Space Propulsion Laboratory were used to perform the experiments in this work. This section details the instruments used for differential electrochemical mass spectrometry, including a residual gas analyzer and electrochemical cell. The overall method was to force ionic liquid propellants to decompose in the electrochemical cell while measuring and identifying the gas produced using the residual gas analyzer. Descriptions of the electrospray thruster and test facility are also provided.

A. Thruster and Test Facility

All experiments are conducted in the Turbovac vacuum test facility within the Space Propulsion Laboratory at MIT. The vacuum chamber, which measures 0.4 m in diameter and 0.8 m in length, is evacuated by a mechanical pump and two turbomolecular pumps to achieve a base pressure of $\sim 10^{-7}$ torr. Chamber pressure is measured using an MKS 972B-71034 pressure transducer. High voltage is generated with a Matsusada AP-3B1-L2 fast high voltage amplifier. Currents are measured using Analog Devices AD210AN isolation amplifiers. All measurement signals are collected with a National Instruments USB-6229 DAQ and logged using custom data acquisition software.

All experiments are conducted using iEPS units developed at MIT. The thruster head, described in detail elsewhere[4,21] , is mounted on a propellant tank with a capacity of about 1 mL, as shown in Figures 2 and 3. The tank consists of a vented outer support shell and a porous Teflon propellant reservoir. The reservoir is permeable to gas, but not liquid, which allows for passive depressurization during chamber pumpdown. Propellant is passively fed from the reservoir to the emitter chip using a paper wick, and the flowrate is mechanically restricted using a Teflon disc.

The propellant is polarized by applying high voltage to a carbon xerogel distal electrode housed within the propellant tank. The potential of the propellant follows that of the electrode. The electrode measures approximately 6 mm in height and 4 mm in diameter, and is wrapped in a sintered glass fiber wick to facilitate continuous fluid transport to the emitter and ensure that the electrode remains in full contact with the propellant throughout operation. As discussed previously, electrochemical reactions are forced to the distal electrode site in order to preserve the emission source. Carbon xerogel offers multiple advantages as a distal electrode material, including its chemical inertness and high specific surface area available to store charge. An SEM image of a xerogel sample is shown in Figure 4. Arestie provides detailed physical characteristics and fabrication processes for the carbon xerogel material developed for use in iEPS.[22]

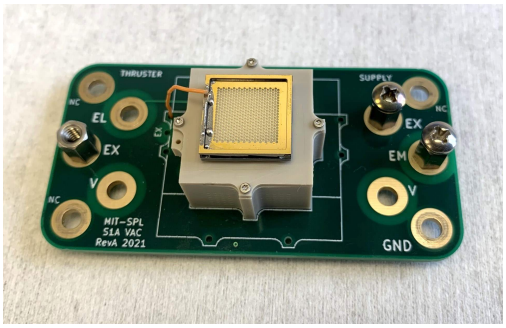

Figure 2. iEPS thruster unit mounted on a circuit board for laboratory testing.

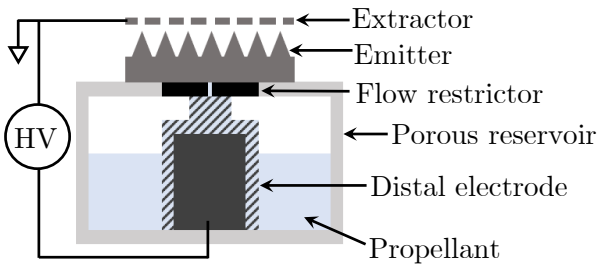

Figure 3. Cross section diagram of an iEPS unit with Teflon flow restrictor and a carbon xerogel distal electrode used to bias the propellant.

B. Electrolytic Cell

Electrochemical cells are devices capable of converting chemical energy to electrical energy (or vice versa) through oxidation-reduction reactions.[23] An electrolytic cell is a type of electrochemical cell that requires an external energetic input to facilitate nonspontaneous chemical reactions. A simplified schematic of an electrolytic cell is shown in Figure 5. The cell consists of a power source and two inert electrodes - a cathode and anode - that are immersed in an ion-conducting electrolyte. A potential difference is applied between the electrodes. Cations in the electrolyte are attracted to the cathode, where they are electrically reduced by accepting electrons. Anions are attracted to the anode and are oxidized, releasing electrons which flow through the external circuit to the cathode.

In this work, we constructed an electrolytic cell using three common electrospray propellants as electrolytes: EMI-BF_4, EMI-CF_3BF_3, and EMI-Im. The cell consists of a glass vial filled with 1.0 mL of each ionic liquid. The vial is sealed with a porous Teflon septum permeable to gas but not liquid. A 3-electrode configuration is used, with a 0.01" platinum reference electrode, and both working and counter electrodes made of 1 mm cylindrical rods of polished graphite. The cell potential is applied to the working electrode (anode) with respect to the reference electrode using a VersaStat 3000 potentiostat. A potentiostat is an instrument used in analytical electrochemistry to precisely control the voltage difference between electrodes and measure the current response of the system.

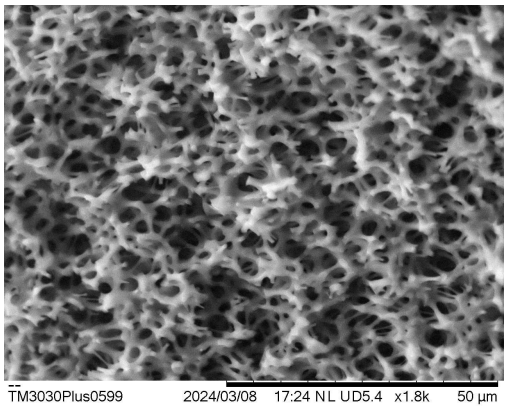

Figure 4. SEM image of carbon xerogel electrode microstructure.

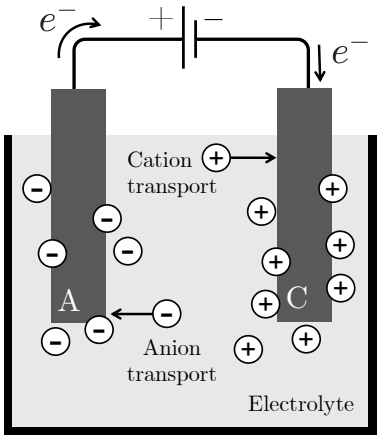

Figure 5. Schematic of a 2-electrode electrolytic cell with an anode (A) and a cathode (C).

C. Residual Gas Analyzer

An ExTorr XT residual gas analyzer (RGA) is used to measure the background species composition in the vacuum chamber. RGAs are mass spectrometers typically used to identify trace amounts of contaminants in high-vacuum systems. Here, it is used to detect gas-phase products of electrochemical reactions. The RGA consists of an electron ionization source and a quadrupole mass spectrometer that filters particles by their mass to charge ratios (m/z). Since its detection range is 1–200 amu (assuming all species are singly-charged), our RGA is capable of detecting EMI, BF_4, and CF_3BF_3 monomers and their fragments. The anion of EMI-Im has a mass outside of this range. More details on the theory and operation of quadrupole mass filters is found in Ref.[24] For all experiments in this work, the RGA is located approximately 15 cm from the source of electrochemical gas (electrospray thruster or electrochemical cell).

The RGA is well-suited to the electrospray test environment because it is noninvasive, relatively sensitive, and compatible with high-vacuum conditions. In the scope of this work, it is used to qualitatively identify new volatile species that emerged due to electrochemical reactions and how they tended to evolve with time. However, limitations exist to the types of measurements that the RGA is capable of taking, and care should be taken in interpreting their readings. In particular, exact quantitative partial pressure measurements are challenging to obtain. The RGA uses electron impact to ionize molecules in the ionization volume of the ion source. Because every molecule has a unique ionization probability based on its collision cross section, the RGA has a different sensitivity to every species. Readings are reported here as approximate partial pressures because they have more physical significance than the detector current, and because many gases are within a factor of 2 sensitivity of nitrogen, the calibration fluid for the RGA. In addition, most RGAs do not have sufficient resolution to distinguish between species with masses within $\pm$ 1 amu - for example, dinitrogen and carbon monoxide appear as the same peak at $m/z = 28$ amu. It can therefore be challenging to conclude what species are present in the system, although it is common practice to make educated guesses based on known contaminants, their physiochemical properties, and their "cracking patterns".[25] Finally, the RGA detection threshold is reported to be 1E-11 torr, although we generally observe signal noise on the order of 1E-10 torr.

IV. Results

A. Identification of Gas-Phase Electrochemical Products

An electrochemical cell, described in Section IIIB, was constructed to identify the gases generated through electrochemical decomposition of three ionic liquids: EMI-BF_4, EMI-CF_3BF_3, and EMI-Im. The cell potential was stepped from 0-9 V in 0.5 V increments. The potential was held constant at each setpoint for 3 minutes, similar to the procedure followed by Masuyama.[26]

The EMI-BF_4 cell progression at various stages in the experiment is shown in Figure 6. The electrochemical window of EMI-BF_4 is reported to be 4.55 V.[16] At cell potentials of 5 V and higher, the propellant visibly reacted with darkly colored deposits forming on the anode and bubbling at the cathode. The rate of product formation increased with the applied cell potential. Initially a clear liquid, the propellant was gradually discolored to a dark brown from the solid deposits created at the anode. Similar results were seen for the EMI-CF_3BF_3 and EMI-Im cells, with visible bubbling at the cell cathodes and deposit formation at the anodes for potentials in excess of the electrochemical window of each liquid.

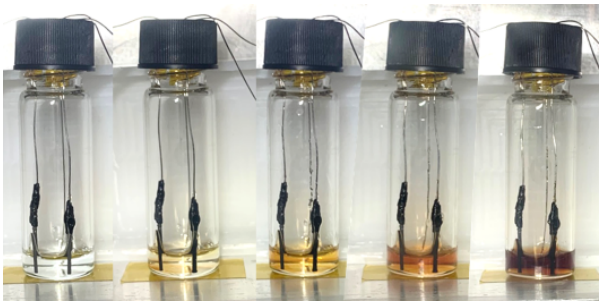

Figure 6. Decomposition of the ionic liquid EMI-BF_4 in an electrolytic cell. Bubbles formed at the cathode (left electrode) while dark brown deposits formed at the anode (right electrode).

RGA mass spectra for the EMI-BF_4 cell are shown as a function of the applied cell potential in Figure 7. The plot is truncated at $m/z = 120$ amu because no strong signals were observed at higher masses. At potentials of 5 V and below, the spectra are nearly identical, and the only peaks visible are those of common residuals found in vacuum systems, such as water ($m/z = 18$ amu), and dinitrogen ($m/z = 28$ amu). At potentials of 6 V and higher, new peaks at heavy mass values emerged and increased in magnitude with the applied potential. The appearance of these peaks were synchronized with the formation of large bubbles at the cell cathode as well as large spikes in the vacuum chamber pressure by nearly an order of magnitude. Therefore, it can be concluded that the new peaks detected in Figure 7 come from gas-phase products of the electrochemical decomposition of EMI-BF_4.

The other ionic liquid cells showed qualitatively similar behavior. For potentials greater than 5 V and 7 V, heavy new mass peaks emerged in the RGA mass spectra for EMI-CF_3BF_3 and EMI-Im respectively. For brevity, the RGA mass spectra at all cell potentials have been omitted here but can be found in Ref.[9] A spectrum for each ionic liquid at an applied potential of 8 V is shown in Figure 8. The plots are truncated at 35 and 115 amu to contain the electrochemical signals only, since no new peaks emerged at masses outside of this range for any of the ionic liquids. "Relative abundance" is defined as the partial pressure of each species normalized by the total chamber pressure. Candidate species have been identified for the most abundant peak in each cluster for all spectra. Following Masuyama's approach,[26] candidates were identified based on the known chemical composition of the ionic liquids and the reported physical stability of each species.

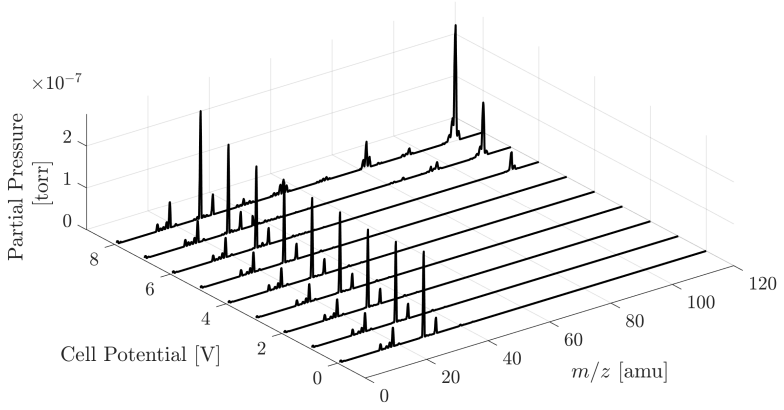

Figure 7. RGA spectra taken at different electrolytic cell potentials. At high cell potentials, new, relatively heavy peaks emerge, representing volatiles formed electrochemically.

For the EMI-BF_4 cell, the largest electrochemical peak appears at $m/z = 111$ amu, the molecular mass of the EMI monomer ($C_6H_{11}N_2$). New peaks are also seen at about 82 and 96 amu. The identities of these species are unknown, but likely fragments of the EMI monomer because fragments of the BF_4 anion ($m/z =$ 86.8 amu) are too light. These results agree with other studies that suggest the cathodic half-reaction in an ionic liquid cell is the reduction of the cation.[10] It should be noted that since the energy of electrons from the RGA ionization source is about 70 eV, it is possible that electron impact could break apart particles in the ionization volume. Cell products could also react with other gases in the chamber before entering the mass spectrometer. Therefore, the heavy peaks shown in Figure 7 are not necessarily the decomposition products of EMI-BF_4, but their presence in the RGA spectra indicates that an electrochemical reaction has occurred. We used peak $m/z = 111$ amu as the "chemical signal" for the gas evolution experiments in Section IVB.

The mass spectrum for the EMI-Im cell is qualitatively very similar to that of the EMI-BF_4 cell. The largest electrochemical peak is again $m/z = 111$ amu, the mass of the EMI monomer. Other peaks are centered at the same mass values, which would be consistent with the same electrochemical products being formed for both ionic liquids. Both spectra are fairly consistent with results from a similar experiment done by Masuyama.[26] Interestingly, the mass spectrum for the EMI-CF_3BF_3 cell in Figure 8 is dramatically different from the other two. The only prominent electrochemical peak is centered at a mass of 69 amu, which corresponds to the mass of the CF_3 group in the anion, or various fragments of the EMI ion.

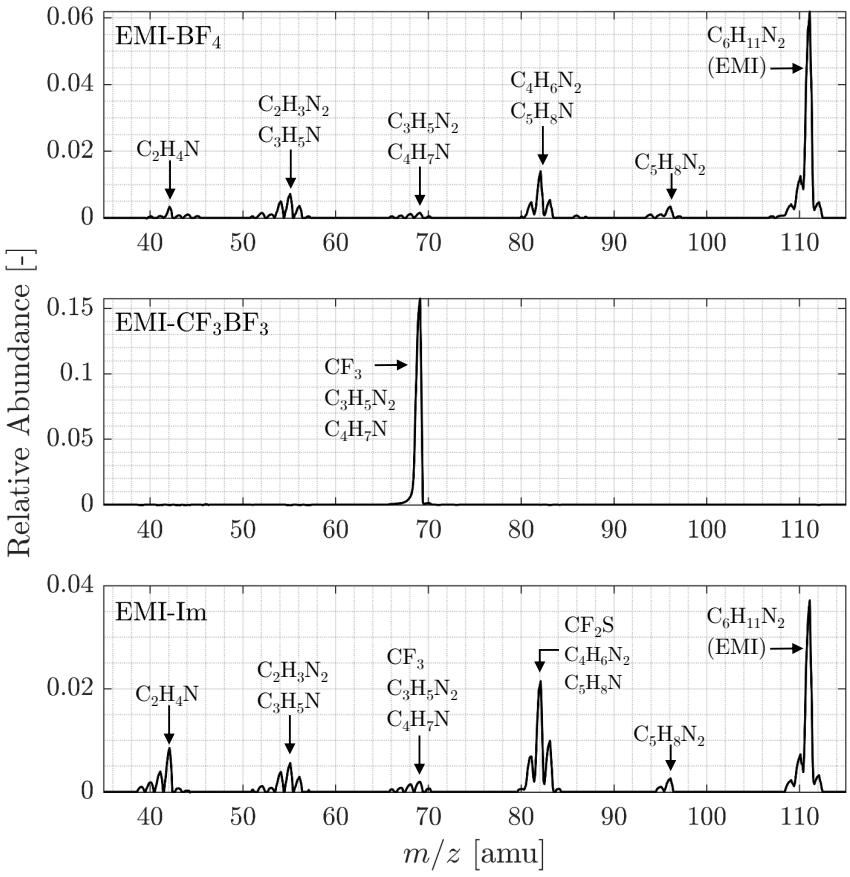

Figure 8. RGA spectra for EMI-BF_4, EMI-CF_3BF_3, and EMI-Im at an applied cell potential of 8V. Peaks in the spectra show the gas-phase species formed electrochemically.

B. Gas Evolution in Electrospray Thrusters

We found that the electrochemically formed volatiles identified in Section IVA are detected independently in previous long-duration electrospray thruster tests.[9] An iEPS electrospray thruster was fired with EMI-BF_4 for 6 hours in the negative polarity at a constant current of about -200 μA. Three chemical signals m/z = 111, 96, and 82 amu measured by the RGA during emission ($t = -6$ to 0 hours) and for 24 hours after thruster shutoff ($t = 0$ to 24 hours) are shown in Figure 10a. An arbitrary signal of m/z = 100 amu is included as a control for comparison. We observed a sharp drop in all signals immediately following thruster shutoff. All chemical signals gradually increased after $t = 0$. Meanwhile, the control signal m/z = 100 amu and practically all others except the chemical signals remained constant. Typically, the Turbovac chamber pressure increases by an order of magnitude while thrusters are firing compared to the base pressure ($\sim$ 1E-6 vs $\sim$ 1E-7). The RGA signal noise increases with chamber pressure, explaining why the control signal m/z = 100 was slightly higher when the thruster was on. The RGA signals at 111, 96, and 82 amu measured during emission could have been generated through processes other than electrochemistry, including thermal decomposition, fragmentation, and/or signal noise. Secondary species from particle-wall collisions are probably not responsible, since recent work shows that the collision byproducts of a $\sim$ 1 keV EMI-BF_4 ion beam are mostly light species less than 60 amu.[27] After thruster shutoff, only electrochemical reactions in the propellant can reasonably explain the increasing abundance of the signals identified independently with an electrolytic cell. The chamber pressure increased from 4.5E-8 torr at $t = 0$ hours to 7.6E-8 torr at $t = 24$ hours, which is consistent with a small amount of gas being generated within the chamber.

At the end of the 24-hour measurement period, the test was repeated following the same procedure. The EMI signal for the first test (Run 1) and the second test (Run 2) are shown in Figure 10b. Both tests show very similar results, confirming that the chemical signals are repeatable and can be attributed to a

real physical process rather than random fluctuations in the chamber or environment. In addition, this result shows that gas evolves in a fairly consistent manner for a given electrospray thruster and set of test conditions.

We then conducted a series of follow-on experiments to investigate the influencers of electrochemical gas evolution. In each test, an iEPS electrospray thruster was fired at a constant current for 6 hours, and RGA spectra were recorded for 24 hours after turning off the thruster. It is not recommended to operate the RGA for several days continuously, so we stopped our measurements at 24 hours. EMI-BF_4 was used as the propellant in all tests. Three parameters were varied in these experiments to examine their effect on the measured gas generation: firing polarity, distal electrode geometry, and emission current.

1. Effect of Firing Polarity

Chemical gas evolution was measured for thrusters fired in the positive mode, negative mode, and in an alternating polarity scheme. All thrusters were fired at a current magnitude of about 200 μA for 6 hours. The alternation period for the dual-polarity test was 30 seconds. Xerogel electrode "A" was used for a negative mode and the dual-polarity test, and the results are shown in Figure 10c. Due to experimental limitations, only about 3 hours of RGA data were obtained for this negative-mode test. Nonetheless, these data are sufficient to capture the main features of the EMI signal evolution after thruster shutoff. Xerogel electrode "B" was used for the positive mode test and a separate negative mode test; these results are shown in Figure 10d.

The EMI signal for the negative and dual-polarity tests (electrode A) show a roughly similar trend with a peak at about 2.5 hours, followed by a gradual exponential decay. The negative-mode signal was almost an order of magnitude greater than the dual-polarity signal. Note that in Figure 10c, the dual-polarity data have been plotted on a separate axis to highlight the similar trends between the two signals despite their difference in magnitude. The EMI signals for the negative and positive mode tests (electrode B) follow a similar increasing trend with a small dip about 10-12 hours after emission stopped. The negative-mode EMI signal was larger than in the positive-mode.

2. Effect of Electrode Geometry

Two different types of distal electrode were investigated: a standard carbon xerogel electrode and a nonporous platinum distal electrode. The platinum distal electrode was 0.01" thick and 0.25" long. A comparison of the two types of electrodes is shown in Figure 9. The same emitter array and propellant reservoir were used in both experiments.

Figure 10e shows a comparison of the EMI signal measured after the thruster was fired with each distal electrode geometry. We observe that the chemical signal is relatively slow and irregular for the xerogel electrode. For the solid platinum electrode, the chemical signals increase rapidly to a peak at about 15 minutes, after which the signal follows a clean exponential decay for the remainder of the measurement period. Likely, the prolonged signal decay was caused by gas diffusing through the porous Teflon reservoir material since the electrode was non-porous.

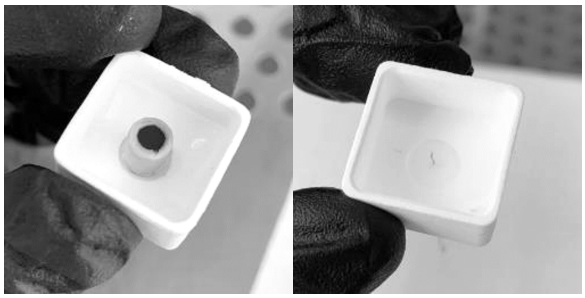

Figure 9. Comparison of iEPS porous Teflon propellant reservoir with a carbon xerogel distal electrode (left) and a solid platinum distal electrode (right).

3. *Effect of Thruster Current*

The effect of thruster current magnitude on chemical gas generation was explored by firing the same thruster at a beam current of -20 μA to compare with our result at -200 μA. The same xerogel electrode was used in both tests. The EMI signals after thruster shutoff for each case are shown in Figure 10f. The EMI signal for the low current case is much less than in the high current case.

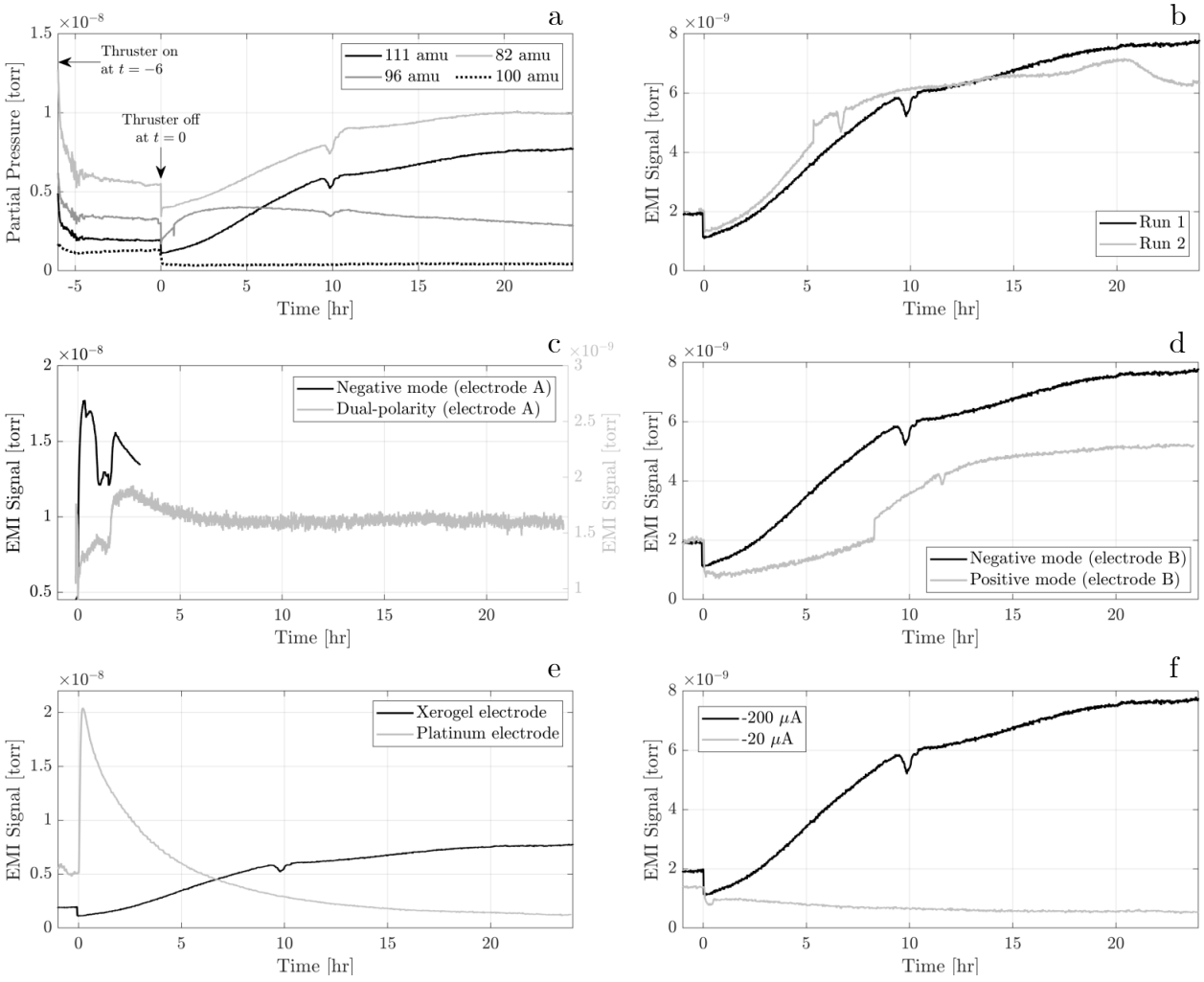

Figure 10. a) Chemical signals 82, 96, and 111 amu measured during and after 6 hours of negative-mode emission, and EMI (111 amu) signal after b) repeated negative-mode emission, c) dual-polarity vs negative-mode emission, d) positive vs negative-mode emission, e) negative-mode emission for a porous xerogel vs solid platinum electrode, f) negative-mode emission at different currents.

V. Discussion

Overall, the experimental results demonstrate that electrochemical reactions can generate gas-phase products in ion electrospray thrusters. These reactions consume some amount of propellant mass, potentially limiting the lifetime and efficiency of the thruster. As shown by the electrolytic cell experiment, the decomposition of the ionic liquid EMI-BF_4 produces both gas-phase and solid-phase products. The most abundant volatiles measured by a residual gas analyzer had masses of 82, 96, and 111 amu, the latter being the molecular mass of the EMI monomer. In independent tests of MIT's iEPS, we detected these same species in increasing abundance for 24 hours *after* 6-hour periods of continuous emission, as shown in Figure 10. Meanwhile, the signals of nearly all other masses remained constant. Moreover, we confirmed that two

key parameters thought to control classical double-layer charging - the electrode geometry and current - were strongly correlated with the amount of chemical gas formed, supporting the hypothesis that electrochemistry at the distal electrode was responsible for the gas.

A. Impact of Electrochemical Phenomena

The occurrence of electrochemical reactions is an unexpected result since obvious visual indicators (e.g. discoloration, tip damage, solid deposits) are rarely observed in routine, short-duration iEPS testing. However, we detected measurable chemical gas despite the use of polarity alternation and a distal electrode. These strategies certainly mitigate but may not altogether prevent electrochemical reactions in electrospray thrusters, which is problematic because gas generation can promote various life-limiting phenomena. For example, positive pressure inside a propellant reservoir could force excessive fluid to the emitter substrate, resulting in flooding during idle periods. Released gas could also promote hazardous electrical discharges.[2,28] The standard mitigation strategies of polarity alternation and high active area electrodes may require further development to prevent electrochemical effects from causing premature thruster failure in the future. This work is relevant as the field continues to work to improve electrospray thruster lifetimes for long-duration operation in space.

Apart from the potential impact to thruster lifetime, electrochemical reactions also affect the overall efficiency of the system since any propellant mass consumed in a reaction cannot contribute to useful thrust. The effect is a reduction of the mass utilization efficiency (η_u), defined as the ratio of ionized exhaust mass flow rate to the total mass flow rate, and historically taken to be 1.[29] We are presently working to quantify the mass utilization efficiency for electrospray thrusters that suffer electrochemical losses.[9] In recent work, Natisin et al. estimate a mass utilization efficiency of about 40%, which is potentially the dominant performance loss for ion electrospray thrusters.[30] This phenomenon is presently unexplained and has drawn interest in studying "anomalous" modes of mass loss. Our results support the hypothesis that electrochemical reactions could be at least partly responsible for this mass loss.

B. Electrochemical Mechanisms

This work focused on gas-phase electrochemical products. However, the formation of solid-phase products in ionic liquid ion sources has also been reported.[1,3,6] We did not observe similar deposits on the thruster hardware or distal electrode in any of our experiments, but it may be possible that small, imperceptible quantities of these species formed within the xerogel electrode microstructure or emitter pores. Experimental methods should be investigated to make this determination since solid deposits could also be problematic for thruster performance and lifetime. Various forms of mass spectrometry have been explored for similar purposes,[31,32] including other in-situ techniques coordinated with differential electrochemical mass spectrometry.[33,34] If careful experimental controls are implemented, the distal electrodes could be weighed before and after a long-duration experiment to determine mass change from chemical residue.

Theory predicts that double-layer charging is an area-driven process, which is consistent with our experimental results. As shown in Figure 10e, a small, relatively flat distal electrode contact created a fast spike in electrochemical gas. The gas formed with the xerogel electrode evolved in a slower, irregular manner, suggesting that the microstructure of the electrode was coupled to the rate and quantity of chemical species formed. This makes sense - as discussed previously, double-layer reactions are triggered once the interfacial electric field (which is dependent on the electrode geometry) reaches a certain threshold. Likely, the chemical reactions took place both at the xerogel electrode surface and deep within its microstructure. The gas signals measured long after emission could then be explained by slow gas evolution within the pores, diffusion out of the pore structure, and/or diffusion out of the Teflon iEPS reservoir.

Figure 10c and 10d show that the iEPS thrusters fired with the same distal electrodes exhibited similar EMI signal trends regardless of the firing polarity. Meanwhile, the pattern and magnitude of negative-mode signals for electrodes A and B are highly dissimilar. This result suggests that the two electrodes possessed different microstructural properties. Standard processes are followed for the fabrication of carbon xerogels used in iEPS and elsewhere. However, it is challenging to precisely measure and control the geometric characteristics of the finished material (e.g. specific area, pore size, porosity, tortuosity). Various methods have been explored to characterize the geometries of intricate porous materials, such as optical imaging,[14] intrusion porosimetry,[35] and electrochemical impedance spectroscopy.[36] Future efforts to standardize the electrodes could potentially investigate these methods.

The basic physical mechanisms responsible for gas being detected after emission are unclear. One possibility is that the propellant began to react at some point during emission after the double-layer breached the electrochemical window of EMI-BF_4. This scenario follows our current understanding of double-layer behavior. Particles of the products formed through these reactions could have been physically obstructed from escaping the electrode microstructure and propellant reservoir during emission by the counterflow of ions (i.e. exhaust mass) traveling through the bulk ionic liquid to the distal electrode site. Once emission stopped, the products may have then been able to diffuse out of the electrode and reservoir. A second possibility is that the electrochemical reactions occurred only after emission. This scenario contradicts our understanding of how electrical double-layers behave, however it may be possible since the reaction products were only detected after emission, including in the case of the solid distal electrode. Further research on double-layer charging in ionic liquid ion sources is required to explain our results.

C. Future Work

With a qualitative understanding of electrochemical processes in electrospray propulsion systems, ample opportunities for future work are opened up. As previously discussed, a better understanding of the physical mechanisms responsible for the observed gas generation is necessary. An experimental path for this is to conduct similar gas generation experiments under a wider set of test conditions. For example, the effects of the firing duration, polarity alternation period, and propellant could be explored, particularly for ionic liquids with much larger or smaller electrochemical stability windows. It remains to be determined whether similar behavior is observed for other electrospray architectures. Pure-ion electrospray thrusters tend to operate at much higher beam currents[4,30] than colloid thrusters.[37] Depending on the distal electrode geometry, slower double layer charging and therefore less electrochemical activity should therefore be expected for electrosprays that operate in the droplet regime.

VI. Conclusion

This work was an exploratory study of how electrochemical reactions could manifest, if at all, in electrospray propulsion systems. In particular, we focused on the formation of gas-phase species, a process that can reduce the efficiency and lifetime of the thruster by consuming useful propellant mass and promoting other life-limiting phenomena. We were able to detect these species in-situ by first identifying the relevant decomposition products for ionic liquid propellants using an electrochemical cell and mass spectrometer, and then measuring the abundance of these species during extended thruster testing. The results suggest that trace amounts of electrochemical gas are likely generated at the distal electrode site after several hours of continuous emission, showing that electrochemical reactions may occur in electrospray systems despite there being no visual signs of degradation. Future work should more closely characterize the physical processes responsible for these reactions and quantify their impact on the efficiency and lifetime of the propulsion system. With this information, more resilient and efficient electrospray thrusters can be developed to benefit a wide range of spacecraft missions.

References

[1]P. Lozano and M. Martinez-Sanchez, "Ionic liquid ion sources: suppression of electrochemical reactions using voltage alternation," *Journal of Colloid and Interface Science*, December 2004.

[2]N. A. Brikner, "On the identification and mitigation of life-limiting mechanisms of ionic liquid ion sources envisaged for propulsion of microspacecraft," Ph.D. dissertation, Massachusetts Institute of Technology, 2015.

[3]S. Castro and J. Fernández de la Mora, "Effect of tip curvature on ionic emissions from taylor cones of ionic liquids from externally wetted tungsten tips," *Journal of Applied Physics*, vol. 105, no. 3, p. 034903, 2009.

[4]D. Krejci, F. Mier-Hicks, R. Thomas, T. Haag, and P. Lozano, "Emission characteristics of passively fed electrospray microthrusters with propellant reservoirs," *Journal of Spacecraft and Rockets*, vol. 54, no. 2, pp. 447–458, 2017.

[5]E. Petro, A. Bruno, P. Lozano, L. E. Perna, and D. Freeman, "Characterization of the tile electrospray emitters," in *Aiaa propulsion and energy 2020 forum*, 2020, p. 3612.

[6]D. G. Courtney, H. Q. Li, and P. Lozano, "Emission measurements from planar arrays of porous ionic liquid ion sources," *Journal of Physics D: Applied Physics*, vol. 45, no. 48, p. 485203, nov 2012.

[7]N. Brikner and P. C. Lozano, "The role of upstream distal electrodes in mitigating electrochemical degradation of ionic liquid ion sources," *Applied Physics Letters*, vol. 101, no. 19, p. 193504, 2012.

[8]S. Z. Shaik, O. Jia-Richards, and P. C. Lozano, "Characterization of a single-polarity electrospray propulsion system," in *37th International Electric Propulsion Conference*, Cambridge, Massachusetts, USA, 06 2022.

[9]S. Z. Shaik, "Single-polarity ion electrospray propulsion," Master's thesis, Massachusetts Institute of Technology, 2023.

[10]M. C. Kroon, W. Buijs, C. J. Peters, and G.-J. Witkamp, "Decomposition of ionic liquids in electrochemical processing," *Green Chemistry*, vol. 8, no. 3, pp. 241–245, 2006.

[11]G. H. Lane, "Electrochemical reduction mechanisms and stabilities of some cation types used in ionic liquids and other organic salts," *Electrochimica acta*, vol. 83, pp. 513–528, 2012.

[12]J. Lu, X. Hua, and Y.-T. Long, "Recent advances in real-time and in situ analysis of an electrode–electrolyte interface by mass spectrometry," *Analyst*, vol. 142, no. 5, pp. 691–699, 2017.

[13]D. Alwast, J. Schnaidt, Y. T. Law, and R. J. Behm, "A novel approach for differential electrochemical mass spectrometry studies on the decomposition of ionic liquids," *Electrochimica Acta*, vol. 197, pp. 290–299, 2016.

[14]K. Masuyama, "Electrochemistry of room temperature ionic liquids with applications to electrospray propulsion," Ph.D. dissertation, Massachusetts Institute of Technology, 2016.

[15]A. B. McEwen, H. L. Ngo, K. LeCompte, and J. L. Goldman, "Electrochemical properties of imidazolium salt electrolytes for electrochemical capacitor applications," *Journal of the Electrochemical Society*, vol. 146, no. 5, p. 1687, 1999.

[16]S. Zhang, X. Lu, Q. Zhou, X. Li, X. Zhang, and S. Li, "Ionic liquids: Physiochemical properties." Amsterdam: Elsevier, 2009.

[17]G. Pettersson, A. Bruno, M. Corrado, B. Medina, D. Krejci, and P. Lozano, "Performance measurement and propellant testing for the step-1 cubesat elecrospray thrusters," in *37th International Electric Propulsion Conference*, Cambridge, Massachusetts, USA, 06 2022.

[18]N. R. Demmons, N. Lamarre, J. K. Ziemer, M. Parker, and D. Spence, "Electrospray thruster propellant feedsystem for a gravity wave observatory mission," in *52nd AIAA/SAE/ASEE Joint Propulsion Conference*, 2016, p. 4739.

[19]A. A. Kornyshev, "Double-layer in ionic liquids: paradigm change?" pp. 5545–5557, 2007.

[20]M. Z. Bazant, "Lecture 34: Transport in porous media," *MIT OpenCourseWare 10.626 Electrochemical Energy Systems*, 2011.

[21]D. S. Freeman, "Design and manufacture of the next generation of ion electrospray thrusters," Master's thesis, Massachusetts Institute of Technology, 2019.

[22]S. M. Arestie, "Porous material and process development for electrospray propulsion applications," Master's thesis, Massachusetts Institute of Technology, 2014.

[23]A. J. Bard, L. R. Faulkner, and H. S. White, *Electrochemical methods: fundamentals and applications*. John Wiley & Sons, 2022.

[24]P. Dawson, "Chapter ii - principles of operation," in *Quadrupole Mass Spectrometry and its Applications*, P. H. DAWSON, Ed. Elsevier, 1976, pp. 9–64.

[25]B. Jenninger and P. Chiggiato, "Cas tutorial on rga interpretation of rga spectra," *CERN Accelerator School: Vacuum for Particle Accelerators*, 2017.

[26]K. Masuyama and P. C. Lozano, "Bimodal propulsion system using ionic liquid propellant for pico- and nano-satellite applications," in *49th AIAA/ASME/SAE/ASEE Joint Propulsion Conference*, 2013.

[27]S. Z. Shaik, A. R. Bendimerad, A. T. M. Tahsin, A. Smith, P. Lozano, and E. Petro, "Characterization of propellant-surface collision byproducts using md simulations and rga measurements," in *AIAA SCITECH 2024 Forum*, 2024, p. 1541.

[28]Y. Fujiwara, "Electrochemical reactions of ionic liquid in vacuum and their influence on ion-beam production by electrospray," *Journal of The Electrochemical Society*, vol. 167, no. 16, p. 166504, nov 2020.

[29]P. Lozano and M. Martinez-Sanchez, "Efficiency estimation of emi-bf4 ionic liquid electrospray thrusters," in *41st AIAA/ASME/SAE/ASEE Joint Propulsion Conference & Exhibit*, 2005, p. 4388.

[30]M. R. Natisin, H. L. Zamora, Z. A. Holley, N. Ivan Arnold, W. A. McGehee, M. R. Holmes, and D. Eckhardt, "Efficiency mechanisms in porous-media electrospray thrusters," *Journal of Propulsion and Power*, vol. 37, no. 5, pp. 650–659, 2021.

[31]E. Markevich, R. Sharabi, V. Borgel, H. Gottlieb, G. Salitra, D. Aurbach, G. Semrau, and M. A. Schmidt, "In situ ftir study of the decomposition of n-butyl-n-methylpyrrolidinium bis (trifluoromethanesulfonyl) amide ionic liquid during cathodic polarization of lithium and graphite electrodes," *Electrochimica Acta*, vol. 55, no. 8, pp. 2687–2696, 2010.

[32]S. Bell, C. Geiger, B. Inbar, M. Pfeifer, and E. Petro, "Novel methods to detect trace quantities of 1-ethyl-3-methylimidazolium tetrafluoroborate," in *AIAA SCITECH 2023 Forum*, 2023, p. 1410.

[33]M. B. M. Concha, M. Chatenet, F. H. Lima, and E. A. Ticianelli, "In situ fourier transform infrared spectroscopy and online differential electrochemical mass spectrometry study of the nh3bh3 oxidation reaction on gold electrodes," *Electrochimica Acta*, vol. 89, pp. 607–615, 2013.

[34]B. B. Berkes, A. Jozwiuk, H. Sommer, T. Brezesinski, and J. Janek, "Simultaneous acquisition of differential electrochemical mass spectrometry and infrared spectroscopy data for in situ characterization of gas evolution reactions in lithium-ion batteries," *Electrochemistry Communications*, vol. 60, pp. 64–69, 2015.

[35]P. A. Webb, "An introduction to the physical characterization of materials by mercury intrusion porosimetry with emphasis on reduction and presentation of experimental data," *Micromeritics Instrument Corp, Norcross, Georgia*, 2001.

[36]J. Song and M. Z. Bazant, "Electrochemical impedance imaging via the distribution of diffusion times," *Physical review letters*, vol. 120, no. 11, p. 116001, 2018.

[37]J. Ziemer, C. Marrese-Reading, C. Dunn, A. Romero-Wolf, C. Cutler, S. Javidnia, T. Li, I. Li, G. Franklin, P. Barela *et al.*, "Colloid microthruster flight performance results from space technology 7 disturbance reduction system," in *International Electric Propulsion Conference (IEPC) 2017*, no. GSFC-E-DAA-TN47585, 2017.